Development 133, 621-629 doi:10.1242/dev.02235

URI-1 is required for DNA stability in *C. elegans*

Christine T. Parusel[1], Ekaterini A. Kritikou[2,*], Michael O. Hengartner[2], Wilhelm Krek[1,†] and Monica Gotta[3,†]

Unconventional prefoldin RPB5 interactor (URI), an evolutionary conserved member of the prefoldin family of molecular chaperones, plays a central role in the regulation of nutrient-sensitive, TOR (target-of-rapamycin)-dependent gene expression programs in yeast. Mammalian URI has been shown to associate with key components of the transcriptional machinery, including RPB5, a shared subunit of all three RNA polymerases, the ATPases TIP48 and TIP49, which are present in various chromatin remodeling complexes, and human PAF1 and parafibromin, which are components of a transcription elongation complex. Here, we provide the first functional characterization of a URI-1 homolog in a multicellular organism and show that the *C. elegans* gene *uri-1* is essential for germ cell proliferation. URI-1-deficient cells exhibit cell cycle arrest and display DNA breaks as evidenced by TUNEL staining and the appearance of HUS-1::GFP foci formation. In addition, *uri-1(lf)* mutants and *uri-1(RNAi)* worms show a p53-dependent increase in germline apoptosis. Our findings indicate that URI-1 has an important function in the mitotic and meiotic cell cycles. Furthermore, they imply that URI-1 participates in a pathway(s) that is associated with the suppression of endogenous genotoxic DNA damage and highlight a role for URI-1 in the control of genome integrity.

KEY WORDS: DNA damage, Germline, Prefoldin, Proliferation

INTRODUCTION

The *uri* gene (unconventional prefoldin RPB5 interactor) was first identified in human cells where URI was found to be part of a multi-protein complex. This complex includes several proteins such as the F-box protein SKP2; the prefoldins (PFDs) STAP1 (SKP2-associating α-class PFD-1), PFD2 and PFD4; the core subunit of RNA polymerase II, RPB5; and the ATPases TIP48 and TIP49, which are components of various chromatin-remodeling complexes. Genetic and biochemical studies in human and in yeast cells have demonstrated that URI is phosphorylated in a TOR-dependent manner and is required for nutrient-sensitive TOR-dependent transcriptional programs (Gstaiger et al., 2003). In contrast to other known PFD family proteins, URI contains additional conserved protein domains and is more than double the size of other PFDs (Cowan and Lewis, 1999; Geissler et al., 1998; Vainberg et al., 1998), indicating that URI might have multiple functions. More recently, URI has been shown to interact with the tumor suppressor protein parafibromin, a component of the PAF1 complex [which is involved in histone methylation and cell cycle control (Yart et al., 2005)].

Cellular proliferation requires the accurate replication of DNA to ensure the viability of cells and the survival of the species. Different types of DNA damage, such as collapsed replication forks (for a review, see Lambert and Carr, 2005) and chromatin-based defects (for reviews, see Ehrenhofer-Murray, 2004; Koundrioukoff et al., 2004), accumulate constitutively during this process and therefore cells have several mechanisms to ensure that the damage is rapidly recognized and repaired to maintain genomic integrity. Repair processes are particularly important in germline cells where any damage can be transmitted to the progeny.

[1]Eidgenoessische Technische Hochschule Zuerich, Institute of Cell Biology, CH-8093 Zuerich, Switzerland. [2]University of Zuerich, Institute of Molecular Biology, CH-8057 Zuerich, Switzerland. [3]Eidgenoessische Technische Hochschule Zuerich, Institute of Biochemistry, CH-8093 Zuerich, Switzerland.

*Present address: Nature Publishing Group, Porters South, 4 Crinan Street, London N1 9XW, UK
†Authors for correspondence (e-mail: monica.gotta@bc.biol.ethz.ch; wilhelm.krek@cell.biol.ethz.ch)

Accepted 5 December 2005

The *C. elegans* germline has been used extensively to dissect the signaling pathways that regulate DNA damage responses. The two germline progenitor cells that are present in newly hatched larvae, will eventually give rise to ~1000 germ cells per gonad arm in the adult hermaphrodite (Riddle, 1997). Germ cell apoptosis and transient mitotic cell cycle arrest are often triggered upon genotoxic stresses such as DNA damage (Ahmed et al., 2001; Gartner et al., 2000) to prevent the propagation of gametes with damaged genomes. DNA damage triggers cell cycle arrest in the mitotic part of the germline, a response that is abrogated in mutants of the DNA damage sensors HUS-1, MRT-2 and RAD-5 (reviewed by Stergiou and Hengartner, 2004). ATM-1 and ATL-1, the homologues of the ATM and ATR kinases, which have been shown to trigger cell cycle arrest upon DNA damage in all eukaryotic cells studied so far, have also been suggested to be key components of the DNA damage signaling in *C. elegans* (Boulton et al., 2002). In the meiotic part of the germline, DNA damage induces p53/CEP-1-mediated apoptosis, which involves the core apoptotic machinery [the anti-apoptotic Bcl2-like protein CED-9, the Apaf1-like adaptor protein CED-4 and the pro-caspase CED-3 (reviewed by Stergiou and Hengartner, 2004)].

In this report, we describe a novel role for URI-1 in the maintenance of DNA stability in the absence of exogenous DNA damage. We show that loss of *uri-1* results in aberrant DNA damage in the *C. elegans* germline. The increased DNA breaks that are induced due to the loss of *uri-1* trigger a HUS-1 response, which is associated with cell cycle arrest in the mitotic germline and p53/CEP-1-dependent apoptosis in the meiotic germline.

MATERIALS AND METHODS

Strains

Standard methods were used for the maintenance and manipulation of *C. elegans* strains (Brenner, 1974). Bristol strain N2 was used as the standard wild-type strain. The following strains were also used: *uri-1(tm939), uri-1(tm939) dpy-5(e61)/dpy-5(e61) unc-14(e57), dpy-5(e61) unc-14(e57), ced-3(n1286), ced-9(n1950), gld-2(q497) gld-1(q485); unc-32(e189)* (Kadyk and Kimble, 1998), *hus-1(op241); unc-119(ed3); opIs34* (Hofmann et al., 2002), *glp-4(bn2), fem-1(hc17)* (Nelson et al., 1978), *fem-3(q20)* (Barton et al., 1987), *glp-1(q231), atm-1(gk186), spo-11(ok79)/nT1[unc-?(n754)let-?], hus-1(op241),* and *cep-1(gk138)*. The *uri-1(tm939)* mutant allele was

isolated and kindly provided by the National Bioresource Project-Japan. Primers used for PCR screening of the *tm939* allele were 5′-CGCG-GATCCATCATGAGCGAACTCTACGTTGC-3′ and 5′-CCGCTCGAGC-GGTCAATTTCTATGCCTGGAAGC-3′. As the homozygous mutant exhibits a sterile phenotype and/or embryonic lethality, it was marked with the recessive *dpy-5* mutation and cultivated as heterozygous *uri-1(tm939) dpy-5(e61)/dpy-5(e61) unc-14(e57)*.

Characterization of brood size

L4 hermaphrodites of the desired genotype were individually cloned onto agar plates and cultured at 25°C. The hermaphrodites were transferred to fresh plates every 24 hours. The brood size of each animal is the sum of non-hatched and hatched progeny.

RNAi analysis

Double-stranded RNA was applied to worms by feeding or injection (Timmons et al., 2001). A L4440 plasmid that contains a fragment of the C55B7.5 gene was used (Fraser et al., 2000). The bacteria were seeded on NGM agar plates containing 6 mM IPTG and 5 μg/ml carbencillin. Worms were added as L1 larvae on the following day and raised at 25°C. Temperature-sensitive strains were raised at 15°C in P0 generation and shifted to 25°C as L1 larvae. Control animals were fed with bacteria carrying an empty L4440 construct. Phenotypes were observed in the P0 and F1 progeny of worms that were fed with the respective dsRNA at the indicated time points.

Northern blot analysis

To prepare RNA, the *fem-1(hc17)*, *fem-3(q20)*, *glp-4(bn2)* and wild-type strains were grown at 15°C, synchronized at the L1 larval stage and afterwards raised at 25°C, the restrictive temperature for the above-mentioned temperature-sensitive mutants. Under these conditions *glp-4(bn2)* (Beanan and Strome, 1992) contains almost no germ cells (~12) and is considered a germline-free animal, *fem-3(q20)* animals produce sperm but no oocytes (Barton et al., 1987) and *fem-1(hc17)* animals generate oocytes but no sperm (Nelson et al., 1978). One day after reaching the L4 larval stage total mRNA was prepared using the TRIZOL (GIBCO) method (Hope, 1999). Total RNA was separated in formaldehyde-agarose gels by electrophoresis, transferred to a Hybond- N^+ membrane and hybridized in ExpressHyb Hybridization Solution (BD Biosciences) according to manufacturer's protocol with a full length ^{32}P-labeled *uri-1* cDNA probe (using the Prime-It II Random Primer Labeling Kit; Stratagene). The amount of total mRNA was normalized using rRNA as standard.

Germline apoptosis and germ cell counts

Apoptotic germ cell corpses were counted by morphology under DIC optics as previously described (Lettre et al., 2004).

Synchronized wild-type L1 larvae were fed on *uri-1(RNAi)* and the vector control L4440(RNAi) plates at 25°C until adulthood. The worms where then transferred every 2 hours to new plates and the F1 generation (also fed on RNAi) was collected and methanol fixed (–20°C for at least 10 minutes) at the indicated time points. Worms were washed twice in PBS, and they were suspended in PBS including DAPI at 0.1 μg/ml for 30 minutes at room temperature. After two washes with PBS 3 μl Vectashield was added to the worms and samples were mounted on slides. Germ cells that were identified by nuclear morphology according to DAPI staining were counted. The different developmental stages of the worms were determined by vulval morphology and differentiation of somatic gonads.

Immunostaining

For the anti-phospho-histone H3 (PH3) staining, one day post-L4 adult gonads were dissected in PBST (0.2% Triton-X) on POLYSINE slide, fixed for 4 minutes in 1% formaldehyde in PBST and freeze-cracked. The slides were transferred to –20°C cold methanol for 6 minutes and washed three times in PBS each time for 5 minutes. They were blocked for 30 minutes in 3% BSA in PBST at 37°C and incubated overnight at 4°C with the rabbit polyclonal anti-PH3 antibody (1:500 in 3% BSA in PBST, Upstate). The next day the gonads were washed 3 times in PBST each for 10 minutes at RT and incubated for 2 hours with the secondary antibody (anti-rabbit cy3, 1:200) in PBST at RT. Gonads where washed three times in PBST each for 10 minutes (0.5 μg/ml DAPI was added in the first wash) and mounted with 3 μl Vectashield per sample for further analysis.

For the anti-RAD-51 staining one day post-L4 adult gonads were dissected in PBS on POLYSINE slide and freeze-cracked. The slides were transferred to –20°C cold methanol, methanol:acetone (1:1) and acetone each for 5 minutes and washed three times in PBS for 5 minutes each. They were blocked for 30 minutes in 3% BSA in PBST (0.05% Triton-X) at 37°C and incubated overnight at 4°C with the rabbit polyclonal anti-RAD-51 antibody (1:1000 in 3% BSA in PBST). The next day, the gonads were washed three times in PBST each for 5 minutes at room temperature and incubated with the secondary antibody as described above. Gonads were washed three times in PBST each for 10 minutes (0.5 μg/ml DAPI was added in the first wash) and mounted with 3 μl Vectashield per sample for further analysis.

DNA breakage detection methods

For the TUNEL (terminal deoxynucleotidyl transferase-mediated dUTP nick end-labeling) assay, which detects DNA strand breaks (nicks) and DNA fragmentation (staggered DNA ends), 1 day post-L4 gonads were dissected in PBS, transferred to a 96-well plate and fixed in 4% formaldehyde in PBS at room temperature for 20 minutes. Gonads were rinsed in PTX (PBS, 0.4% Triton X-100) three times and incubated in 100 mM sodium-citrate, 0.1% Triton X-100 at 65°C for 20 minutes, followed by two washes in PTX. Gonads were then incubated for 30 minutes at room temperature in 0.1 M Tris/HCl (pH 7.5) containing 3% BSA and 20% normal bovine serum. The gonads were rinsed twice with PBS at room temperature and excess fluid was drained off. Gonads were afterwards incubated in TUNEL reaction mixture (Roche) at 37°C for 1.5 hours. The reaction was stopped by washing the gonads three times in PTX. DAPI (1 μg/ml) was added into each well for 5 minutes within the second washing step. Vectashield (3 μl) was added to each sample and gonads were mounted on to a cover slip for further analyses. The HUS-1::GFP foci and their nuclear re-localization following DNA damage were scored as previously described (Hofmann et al., 2002).

RESULTS

Loss of *uri-1* function results in sterility

We named the *C. elegans* gene *C55B7.5 uri-1* based on sequence homology and conserved protein-protein interactions with members of the human URI complex. Alignment of *Homo sapiens*, *Drosophila melanogaster*, *Caenorhabditis elegans*, *Saccharomyces cerevisiae* and *Arabidopsis thaliana* URI orthologs reveals three highly conserved regions, termed the PFD domain, the RPB5-binding region and the URI box (Gstaiger et al., 2003) (Fig. 1A). We obtained a *uri-1(tm939)* deletion mutant that lacks the second α-helix of the PFD domain and the entire RPB5-binding region. Furthermore, this deletion places the remaining 3′ coding region out of frame (Fig. 1A).

Phenotypical analysis revealed that loss of *uri-1* function causes multiple and variable somatic defects such as protruding vulva (8%±3, *n*=200), rupture (23%±21, *n*=200), embryonic lethality (8%±3, *n*=200), path-finding defects (12%±8, *n*=73), molting problems (8%±4, *n*=200) and L3 larval arrest (46%±6, *n*=41). However, the most penetrant phenotype that is observed upon loss of *uri-1* function is sterility. In this report we characterize the germline defects observed in *uri-1(lf)* mutant and *uri-1(RNAi)* worms.

The homozygous *uri-1(lf)* mutants and the progeny of worms fed with *uri-1* dsRNA [referred to as *uri-1(RNAi)*F1] develop into sterile adults (Table 1), indicating that URI-1 is essential for fertility. Both the *uri-1(lf)* mutants and the *uri-1(RNAi)*F1 develop a small germline because of a severe reduction in germ cell number (Fig. 1B and Table 1). This dramatic reduction in germ cell number is not due to increased apoptosis as depletion of *uri-1* in an apoptosis-deficient

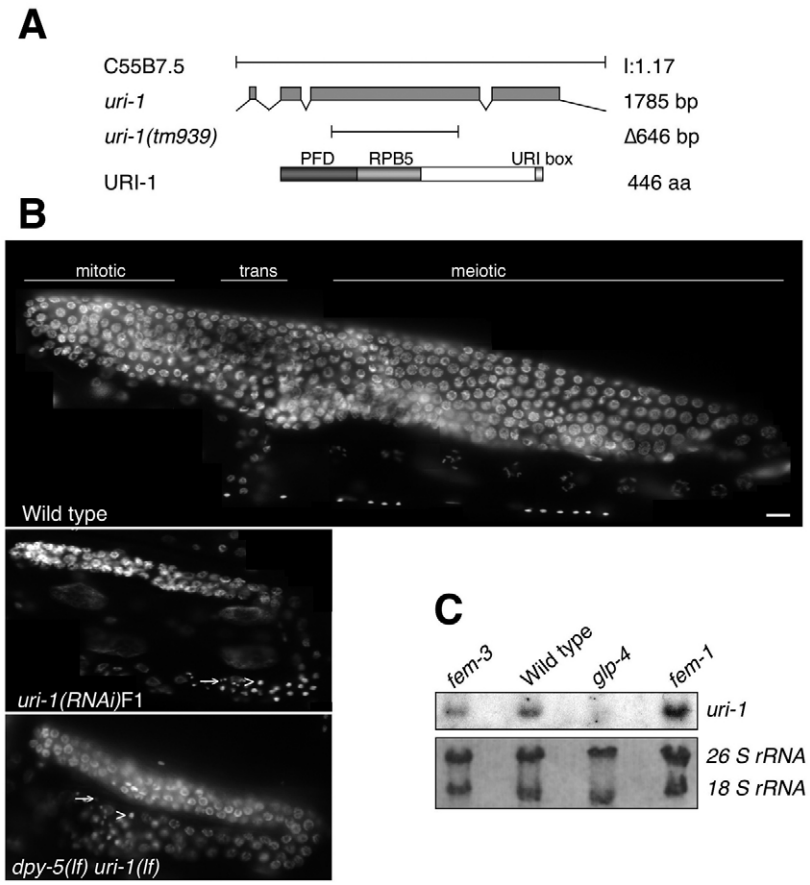

Fig. 1. Characterization of *uri-1* in *C. elegans*. (**A**) Genomic structure of *C. elegans uri-1* (C55B7.5) and *uri-1* deletion mutant *(tm939).* URI-1 encodes a 446 amino acid protein with a putative prefoldin domain (PFD), a direct binding site for the common subunit of all three RNA polymerases RPB5 (RPB5) and the URI-1 box depicted below. (**B**) Images from wild-type adult hermaphrodites, *uri-1(RNAi)*F1 and homozygous *uri-1(tm939)* adult hermaphrodites raised at 25°C and stained with DAPI. Arrows indicate haploid sperm and arrowheads indicate spermatids. Anterior is towards the left and dorsal is towards the top throughout. Scale bar 10 μm. (**C**) Northern blot was performed as described in the Materials and methods and shows that *uri-1* is a germline-enriched transcript expressed in both types of gametes. Ribosomal RNA was used as loading control.

strain also results in a small germline (see Table S2 in the supplementary material). Male *uri-1(RNAi)*F1 animals also suffer from a reduction of germ cells (data not shown), indicating that the function of URI-1 is sex independent.

To investigate whether *uri-1* mRNA is expressed in the germline, we performed northern blot analysis using synchronized wild-type adult worms and mutants with germline defects (Fig. 1C). *uri-1* RNA transcript is detected in worms with masculinised [*fem-3(q20)*] and femininised [*fem-1(hc17)*] germlines but not in *glp-4(bn2)* worms that lack nearly the entire germline. Therefore, consistent with a function in germline development, *uri-1* is a germline enriched transcript that is expressed in both types of gametes.

In wild-type hermaphrodites, the first germ cells that enter the meiotic cycle in each gonad arm (~40) differentiate as primary spermatocytes, then secondary spermatocytes, spermatids and finally form activated spermatozoa (~160). Thereafter, a switch in sexual fate occurs so that all germ cells develop as oocytes (Riddle et al., 1997). A complete lack of oocytes is observed in *uri-1(lf)* mutants and this phenotype is fully penetrant. About 35% (*n*=30) of *uri-1*-depleted germlines do not show any sign of gametogenesis and when gametogenesis occurs it leads to the development of sperm but no oocytes in the corresponding gonads. However, the spermatocytes do not always complete the meiotic divisions, because both spermatocytes (Fig. 1B, arrowheads) and mature sperm (Fig. 1B, arrows) were observed in the gonads of adult hermaphrodites. Moreover, the amount of sperm in the adult germlines of homozygous *uri-1(lf)* mutants is reduced (13±10, *n*=10) compared with wild type (~160).

Table 1. Analysis of brood size, fertility and germ cell number of *uri-1(RNAi)* and *uri-1(tm939)* hermaphrodites at 25°C

Genotype	Brood size	Percentage sterility	Germ nuclei per gonad arm
Wild type	213±39 (*n*=20)	0 (*n*=20)	325±31 (*n*=10)
uri-1$^{+/-}$	74±32 (*n*=20)	0 (*n*=20)	n.d.
uri-1$^{-/-}$	0±0 (*n*=20)	100 (*n*=20)	85±24 (*n*=20)
+/+ (mother *uri-1*$^{+/-}$)	92±25 (*n*=20)	0 (*n*=20)	n.d.
uri-1dpy-5/dpy-5unc-14	55±27 (*n*=30)	0 (*n*=30)	238±32 (*n*=10)
uri-1dpy-5$^{-/-}$	0±0 (*n*=30)	100 (*n*=30)	67±14 (*n*=20)
*uri-1(RNAi)*P0	40±23 (*n*=20)	0 (*n*=20)	278±31 (*n*=10)
*uri-1(RNAi)*F1	3±9 (*n*=30)	87 (*n*=30)	89±63 (*n*=110)

Data are mean±s.d.; *n*=number of animals analyzed.

The adults arising from feeding L1 larvae with *uri-1(RNAi)* (referred to as (*uri-1(RNAi)*P0) display a reduced brood size compared with wild type. Moreover, the germ cell number of these animals is reduced to 73% of the wild-type number (Table 1). Heterozygous *uri-1* hermaphrodites were also subfertile with significantly decreased brood size (Table 1). This shows that URI-1 is haplo-insufficient in ensuring normal germ cell number and brood size. Interestingly, wild-type worms arising from an *uri-1*$^{+/-}$ heterozygous mother give rise to approximately half of the brood size of wild-type worms from a wild-type mother, indicating that zygotically provided URI-1 is insufficient for its role in germline cells and that *uri-1* has to be maternally supplied to ensure normal brood size.

The observation that homozygous *uri-1(lf)* mutants have defects in oogenesis and spermatogenesis, but the heterozygous worms appear normal, indicates that these processes are less sensitive to the loss of *uri-1* levels than are brood size and overall germ cell number.

*uri-1(RNAi)*F1 animals contain an average of 89 germ cells (Table 1). However, the most severely affected animals of the *uri-1(RNAi)*F1 contain only few germ cells (around 18) without any visible gametes, most probably reflecting a stronger loss of URI-1 function.

In conclusion, our data provide the first evidence of a functional role of URI-1 in oogenesis, spermatogenesis, regulation of germ cell number, fertility and germline viability.

URI-1 is required for proliferation of germ cells

As the *uri-1* mutant germlines are smaller because of a severe reduction in germ cell number, we wondered whether URI-1 might have a role in germ cell proliferation. As a hermaphrodite develops from the L1 larval stage to adulthood, the number of somatic cell nuclei roughly doubles (556 to 1090) and the number of germ cells increases from 2 to 2000 germ cells per gonad (Riddle et al., 1997). Germline cells located at the distal end of the gonad arm constitute a proliferating stem cell population. During the larval development of *C. elegans*, the number of germ cells gradually increases, up to the L3 larval stage, when a transition occurs to a period of rapid proliferation (Capowski et al., 1991). Therefore, germline development requires extensive proliferation of cells and URI-1 might be required for germline development because of a role in germ cell proliferation.

A time course analysis of germline development in wild-type worms compared with *uri-1(RNAi)*F1 worms revealed that the rapid increase in germ cell number at the end of the L3 larval stage does not occur in the *uri-1(RNAi)*F1 animals (Fig. 2A). This defect led to a significant difference in germ cell number between *uri-1*-depleted and wild-type worms.

To confirm that *uri-1* is required for germ cell proliferation, we performed *uri-1(RNAi)*F1 in *gld-2(q497) gld-1(q485)*double mutants, which have an over-proliferative germline that contains mainly mitotic cells, owing to meiotic entry defects (Hansen et al., 2004; Kadyk and Kimble, 1998). Loss of *uri-1* in the *gld-2(q497) gld-1(q485)*double mutant suppresses the over-proliferation defect, and gives rise to small germlines with a dramatically reduced cell number (Fig. 2B). Therefore, our data indicate that *uri-1* is required for proliferation of mitotic germ cells.

Cell cycle progression is inhibited in the homozygous *uri-1(lf)* mutant

To further investigate the potential effect of loss of *uri-1* function on cell cycle progression, we examined the nuclear morphology of germline cells in wild-type, *uri-1(lf)* and *uri-1(RNAi)*F1 animals stained with DAPI and with the anti-phospho-histone H3 antibody (PH3), which labels metaphase and telophase cells in the *C. elegans* germline (Hsu et al., 2000; Wei et al., 1999). The DAPI staining revealed the enrichment of nuclei that were arrested at two naturally occurring stages of the cell cycle. First, some nuclei have condensed chromosomes that are not yet aligned to the metaphase plate and are not labeled by the anti-PH3 antibody (Fig. 3A, see arrowheads). This morphology has been described as nuclei in the G2/M phase and could represent G2, prophase or prometaphase nuclei. A similar morphology has been observed in the germline of *hoe-1(RNAi)*-treated animals and has been proposed to represent prometaphases (Smith and Levitan, 2004). Second, *uri-1*-depleted worms also show an enrichment of nuclei that display a metaphase-like morphology and are labeled by the anti-PH3 antibody (Fig. 3B). These nuclei might have escaped the prometaphase-like block and progressed to the next phase of the cell cycle where they finally arrest. This type of cell cycle arrest has been observed in the gonads of the progeny of animals deficient for both the DNA helicase RecQ and topoisomerase IIIα (Kim et al., 2002), which exhibit extensive DNA breakage.

As mentioned above, some germlines are less affected than others after reduction of the URI-1 function. In germlines that contain gametes, we observe spermatids that are also stained with the PH3 antibody, indicating an additional cell cycle block at the M-phase of spermatocyte meiosis I (Fig. 3C) (Golden et al., 2000). This phenotype is unlikely to reflect a role for URI-1 in spermatogenesis, because RNA-mediated inactivation of *uri-1* in the *glp-1(q231)* mutant [in which germ cells enter meiosis early and consequently proliferate far less than in wild-type worms (Austin and Kimble, 1987)] suppresses the URI-1 phenotype, and gives rise to the *glp-1* phenotype without any visible defects in spermatogenesis (see Fig. S1 and Table S1 in the supplementary material). We therefore propose that the defect in spermatogenesis in the URI-1-deficient germlines is a consequence of the cell proliferation defect rather than a direct effect of URI-1 on spermatogenesis.

So far, our data show that loss of URI-1 activity leads to cell cycle blocks that occur in both mitotic and meiotic cells. The suppression of the *uri-1(RNAi)*F1 sperm phenotype by *glp-1(lf)* and the proliferation defect of *uri-1(RNAi)*F1 germlines in the *gld-2(lf)gld-1(lf)* double mutants indicates an important function of URI-1 in mitotic cells.

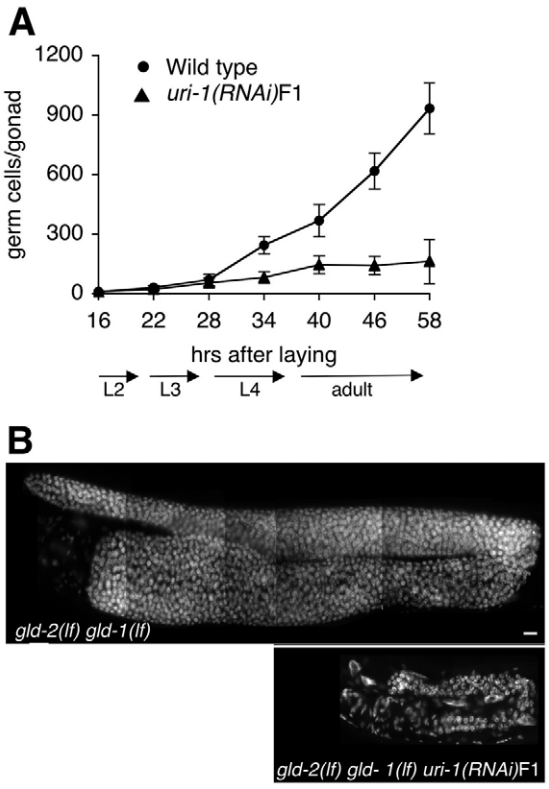

Fig. 2. *uri-1(lf)* mutants have defects in germ cell proliferation. (**A**) Number of germ nuclei per gonad arm in *uri-1(RNAi)*F1 (n=25) and wild-type (n=25) worms. Progeny of staged animals were synchronized by letting the P0 generation to lay eggs for 2 hours, fixed at the indicated time points and stained with DAPI. Germ cells identified by their DNA morphology were counted. Error bars represent s.d. (**B**) Images of *gld-2(lf) gld-1(lf)* (top) and *gld-2(lf) gld-1(lf) uri-1(RNAi)*F1 (bottom) gonads. Loss of URI-1 results in reduction of mitotic germ cells. For both images, anterior is towards the left and dorsal towards the top. Scale bar: 10 μm.

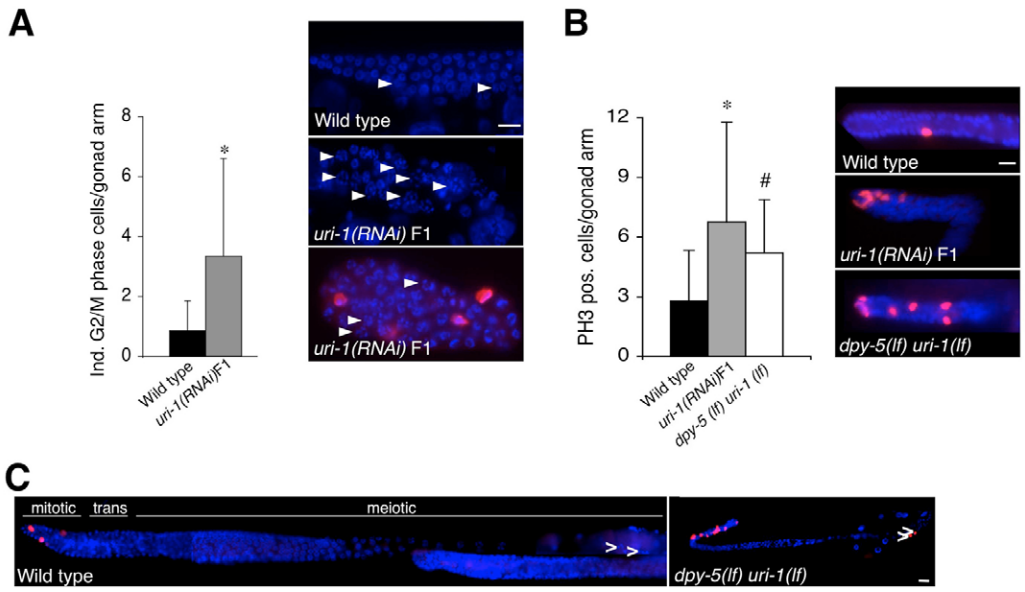

Fig. 3. Loss of URI-1 blocks cell cycle progression in the *C. elegans* germline. (**A**) (Left) Quantification of G2/M phase cells in untreated wild-type (*n*=35, dark) and *uri-1(RNAi)*F1 (*n*=35, grey) synchronized adult hermaphrodites (*$P=5.2\times10^{-5}$). Error bars represent s.d. (Right) DAPI and PH3 staining of the distal part of the germline of a *uri-1(RNAi)F1* and a wild-type worm. The arrowheads indicate mitotic germline cells with apparently condensed chromosomes and different extent of enlargement. This DNA morphology accumulates in germlines upon loss of *uri-1* function and resembles prometaphases which are not recognized by the PH3 antibody (Cy3). Scale bar: 10 μm. (**B**) (Right) Staining with anti-phospho-histone H3 antibody (Cy3) of germ cell nuclei (visualized with DAPI) in the distal region of the gonad of the indicated strains. (Left) PH3-positive nuclei were counted per gonad arm in synchronized adults *uri-1(tm939)* homozygous (*n*=24), *uri-1(RNAi)*F1 (*n*=65) and wild type (*n*=65, Student's test *$P=7.9\times10^{-8}$, #$P=1.0\times10^{-4}$). Scale bar 10 μm. Error bars indicate s. d. (**C**) Anti-PH3 (Cy3) and DAPI staining of a homozygous *uri-1(lf)* mutant and wild-type gonads. Arrowheads indicate sperm. Scale bar: 10 μm. Anterior is towards the left and dorsal is towards the top.

Loss of *uri-1* function results in increased DNA breaks

Block at the G_2/M border is often due to activation of the DNA checkpoint machinery by damaged or incompletely replicated DNA (for a review, see Hartwell and Weinert, 1989). Because we observed a mitotic cell cycle block in the germline of the homozygous *uri-1* mutants, we used three independent assays to investigate whether this block is triggered by damaged DNA.

First, we performed TUNEL staining, which labels DNA strand breaks and DNA fragmentation. In the small germline of the homozygous *uri-1(lf)* mutant and *uri-1(RNAi)*F1 animals, a significantly increased TUNEL staining was observed. As shown in Fig. 4A, some cells show up to 10 TUNEL-positive foci in the germlines of *uri-1*-depleted animal.

Second, we stained *uri-1* depleted worms with antibodies to RAD-51 which has been shown to bind double strand breaks (DSBs) (Alpi et al., 2003; Reddy and Villeneuve, 2004). Anti-RAD-51 staining detected an increased number of DNA breaks in *uri-1(RNAi)*F1 germlines compared with wild type, indicating that *uri-1* depletion results in increased formation of DSBs. It has been demonstrated that the *C. elegans* type II topoisomerase SPO-11 is required to generate meiotic DSBs (Dernburg et al., 1998). We therefore wanted to determine if induction of DSBs requires SPO-11 function. As shown in Table 2, loss of *uri-1* in this mutant background results in an enhancement of DSBs, indicating that a subset of *uri-1(lf)*-induced DSBs are SPO-11 independent.

As a third assay we looked at HUS-1 foci. The checkpoint gene *hus-1* is known to be required for DNA damage-induced cell cycle arrest and apoptosis. HUS-1::GFP localizes diffusely in proliferating germ nuclei under normal conditions. In response to DNA damage, HUS-1::GFP re-localizes in the nucleus and concentrates at distinct nuclear foci that overlap with chromatin believed to be sites of DNA breaks (Hofmann et al., 2002). To test whether the *uri-1(lf)*-induced DNA damage could be detected by the checkpoint machinery, we performed *uri-1(RNAi)* in the HUS-1::GFP strain. *uri-1(RNAi)* resulted in the formation of nuclear HUS-1::GFP foci in the germline (Fig. 4B), consistent with the results obtained with the TUNEL assay and the anti-RAD-51 staining.

Our results clearly show that in the absence of exogenous DNA damage stimuli, loss of URI-1 function results in the formation of DNA breaks. This defect results in the activation of the cellular DNA damage sensing machinery in the germline, as indicated by the formation of HUS-1 foci.

HUS-1 and ATL-1 are required for the cell cycle arrest caused by *uri-1* depletion

Studies in yeast and human cells characterized Hus1 as a sensor of DNA damage that functions in concert with the checkpoint control proteins ATM and ATR to regulate the G_2/M transition (for a review, see Helt et al., 2005). As DSBs in the germline are known to activate

Table 2. Quantification of RAD-51 foci in the indicated genetic backgrounds

Genotype	0-15 cell diameters
Wild type	0.06±0.03 (0-2), *n*=17 (880)
*uri-1(RNAi)*F1	0.35±0.2 (0-10), *n*=15 (583)
spo-11	0.06±0.03 (0-2), *n*=5 (269)
*spo-11;uri-1(RNAi)*F1	0.23±0.09 (0-8), *n*=10 (381)

Mean±s.d. of RAD-51 foci per nucleus are listed and the minimum-maximum number of foci per nucleus are given in brackets. *n*=number of gonads scored. The total number of nuclei is in brackets. The nuclei within a 15 nuclei radius from the distal tip cells were scored.

the cell cycle checkpoint machinery, we investigated if this DNA damage signaling pathway is activated in response to *uri-1* depletion leading to the mitotic cell cycle arrest described above. To address this issue, we depleted *uri-1* in the *hus-1(lf)* mutant strain and analyzed the DAPI stained germlines of *hus-1(op241); uri-1(RNAi)*F1 animals. As shown in Fig. 5A, inactivation of the *hus-1* cell cycle checkpoint gene prevents *uri-1(RNAi)*-induced enrichment of germ cell nuclei blocked at the G_2/M transition. Interestingly, although depletion of the *atm-1* gene had no effect (data not shown), depletion of *atl-1*, the *C. elegans* homolog of ATR, in the apoptosis-deficient *ced-3* strain also resulted in rescue of the *uri-1*-induced cell cycle arrest, phenocopying the rescue observed in the *hus-1;uri-1(RNAi)*F1 germline (Fig. 5B). The observation that inactivation of the checkpoint genes *atl-1* and *hus-1* rescues the cell cycle arrest observed in *uri-1*-depleted worms indicates that this phenotype is mediated by the *hus-1/atl-1* checkpoints of the *C. elegans* DNA damage signaling pathway. However, the decrease in germ cell number (see Fig. 5) and the sperm defect observed in *uri-1*-depleted germlines (data not shown) are not suppressed by loss of *hus-1* or *atl-1*, indicating that loss of URI-1 induces cell proliferation defects that are both *hus-1/atl-1* dependent and independent.

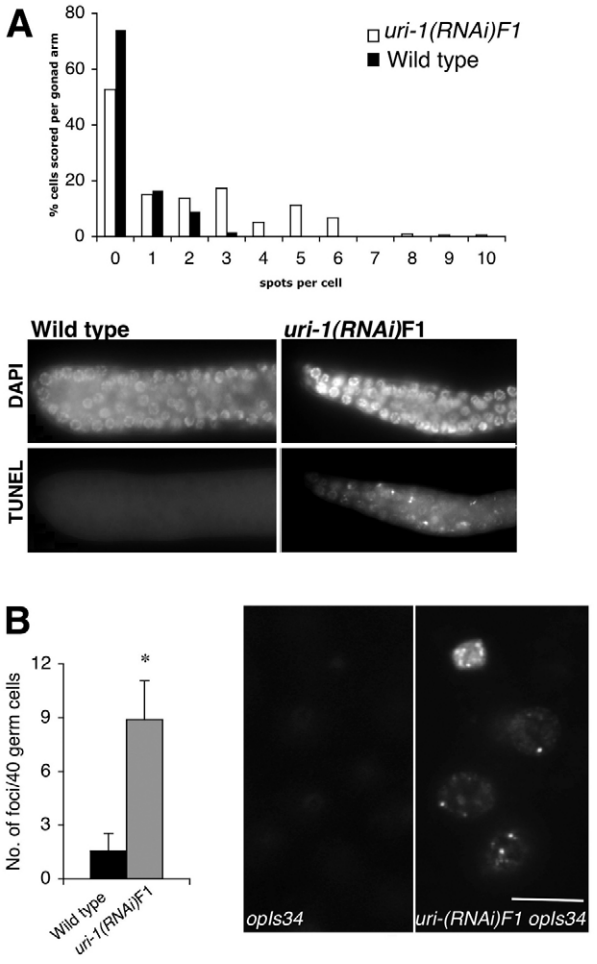

Fig. 4. Accumulation of DNA breaks in the adult hermaphrodite germline due to loss of *uri-1* function. (**A**) (Top) Histograms depicting quantification of TUNEL foci in *uri-1(RNAi)*F1 (n=10) and wild-type (n=10) gonads at 25°C. The nuclei within a 15 nuclei diameter radius from the distal tip cell were scored. Each column represents the percentage of nuclei that contain a defined number of foci. (Bottom) TUNEL staining in wild-type and *uri-1* germlines is shown. Anterior is towards the left and dorsal is towards the top. (**B**) Quantification (left) of the HUS-1::GFP foci in *uri-1(RNAi)*F1 (gray) and control RNAi (black) in *hus-1(op241); unc-119(ed3); opIs34* mitotic germ cells (n=*55* for each, *P=3.4×10^{-43}) and image of germ nuclei (right) showing the relocalization of HUS-1::GFP. OpIS34 is a HUS-1::GFP integrated line. Error bars represent s.d. Scale bar: 5 μm.

Loss of *uri-1* function sensitizes meiotic cells to *cep-1*-dependent apoptosis in the absence of exogenous DNA damage

As *uri-1(lf)* leads to increased DNA damage, we investigated whether this would result in enhanced apoptosis. Apoptosis in the *C. elegans* germline can be visualized under DIC optics – apoptotic cells look like small refractile discs – or with the vital stain Acridine Orange (AO). The heterozygous *uri-1* mutant and *uri-1(RNAi)*P0 worms show an approximately threefold higher AO staining (data not shown) and threefold higher number of germline apoptotic corpses (*gla* phenotype) in their meiotic region compared with wild-type worms (Fig. 6A). The AO staining and the high number of apoptotic corpses that were observed indicate that apoptosis is increased in the germline of these animals. This *gla* effect of *uri-1(RNAi)*P0 is completely suppressed by *ced-9(gf)* and a strong loss of function in *ced-3*, confirming that the cell death observed in the heterozygous *uri-1* mutant and *uri-1(RNAi)*P0 animals is of apoptotic nature (Fig. 6A). To investigate whether the increased apoptosis results from a DNA damage response, we depleted *uri-1* in *cep-1(lf)* mutant worms. CEP-1 is the homolog of the tumor suppressor protein p53 and is known to be required for DNA damage-induced germ cell apoptosis (Schumacher et al., 2001), but dispensable for physiological germ cell death or somatic cell death (Schumacher et al., 2001). The *gla* phenotype of *uri-1(RNAi)*P0 is completely suppressed in the *cep-1(lf)* background (Fig. 6B). This indicates that the *gla* phenotype in *uri-1* animals is due to DNA damage-induced activation of CEP-1. Therefore, reduction of the *uri-1* gene sensitizes meiotic germ cells to *cep-1*-mediated DNA damage-induced germ cell apoptosis in the absence of exogenous DNA damage.

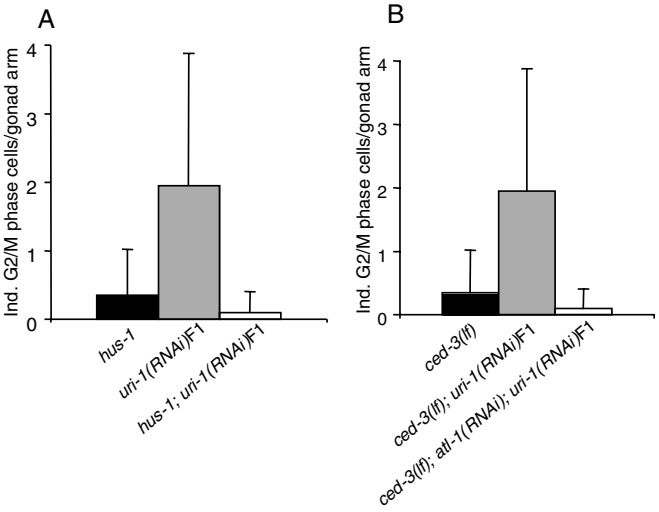

Fig. 5. Depletion of *hus-1* and *atl-1* rescues the cell cycle arrest observed in *uri-1(lf)* worms. Quantification of cells at the G2/M border per gonad arm in the distal region of synchronized *uri-1(RNAi)*F1 in the indicated genotypes in adult hermaphrodites (n=10 each). The number of germ nuclei per gonad arm was 91.3±24.0 in *hus-1; uri-1(RNAi)*F1 (**A**) and 98.8±22.9 in *ced-3(lf); atl-1(RNAi); uri-1(RNAi)*F1 (**B**). Error bars indicate s.d.

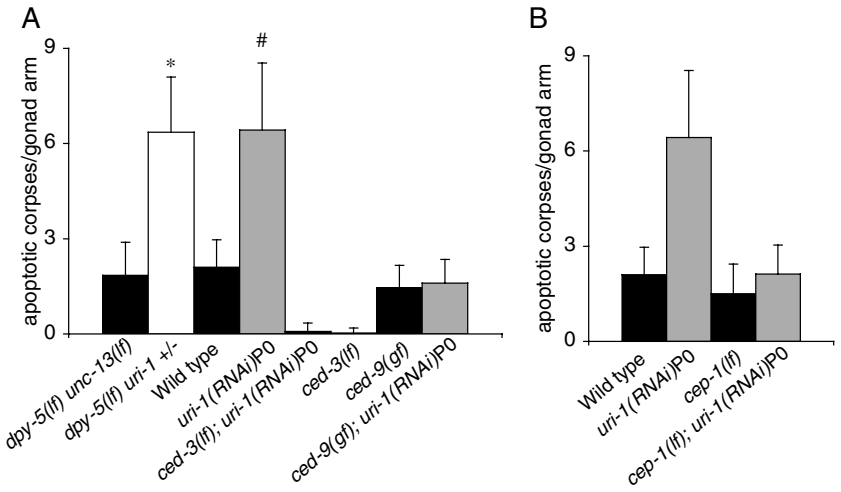

Fig. 6. Effect of *uri-1* depletion on meiotic cells. (**A**) Loss of *uri-1* sensitizes meiotic germ cell to apoptosis. Apoptotic germ cell corpse numbers in the heterozygous *uri-1* mutant and *uri-1(RNAi)P0* animals (n=40 each) reveal a *gla* phenotype, which is completely suppressed by mutations in the apoptotic pathway components *ced-3(lf)*and *ced-9(gf)* ($^{*}P=3.0\times10^{-20}$, $^{\#}P=2.3\times10^{-19}$). Error bars represent s.d. (**B**) Apoptotic germ cell corpse counts in wild-type and *cep-1* germlines of *uri-1(RNAi)P0* and control animals (n=40 each) reveal that the *gla* phenotype that is associated with loss of URI-1 is completely suppressed by loss of the DNA damage sensor *p53* (*C. elegans cep-1*). Error bars represent s.d.

DISCUSSION

In this work we investigated the function of URI-1 in *C. elegans*. We found that *uri-1* homozygous animals develop into sterile adults with a small germline. This severe reduction in germ cell number is due to a defect in cell proliferation. Consistent with the defect in cell proliferation, we observe a cell cycle arrest, which appears to be due to DNA damage as it is suppressed by inactivation of the cell cycle checkpoint genes *hus-1* and *atl-1*. In addition, we show that meiotic cells also display a meiotic cell cycle arrest observed in developing sperm. Finally, we find that DNA damage induced p53-mediated apoptosis is enhanced in the heterozygous mutant. We therefore propose that URI-1 participates in one or more cellular processes, which lead, directly or indirectly, to increased DNA breaks, thereby causing cell cycle arrest (see model in Fig. 7). As the small germline phenotype is not rescued by releasing the cell cycle block upon inactivation of the *C. elegans* homologs of ATR and HUS-1, URI-1 might be required for *hus-1*/*atl-1*-dependent and -independent processes in cell proliferation.

How could URI-1 ensure DNA stability? The amount of DNA breaks present in the *uri-1(RNAi)*F1 germ cells (detected with HUS-1::GFP) is comparable with wild-type worms treated with low dose (5-10 gray) of γ-irradiation (Hofmann et al., 2002). This highlights the severity of the endogenous damage caused by the loss of URI-1 function. The increased numbers of HUS-1::GFP foci formation, the inhibition of mitotic cell cycle progression and the p53-dependent apoptosis indicate that sensing, transduction and execution of DNA damage signals are functional in URI-1 depleted worms. We propose that URI-1 is involved in preventing and/or repairing endogenous, genotoxic DNA damage to maintain genome integrity.

Endogenous DNA breaks can arise from replication errors, repair intermediates and alterations in chromatin remodeling (for reviews, see Abraham, 2001; Koundrioukoff et al., 2004; Lindahl and Wood, 1999; Osborn et al., 2002; Sancar et al., 2004). Several links between DNA repair, replication and chromatin remodeling have been established (Morrison and Shen, 2005; Shen et al., 2000). For example, PCNA has been shown to be involved in chromatin remodeling, replication and repair (for a review, see Majka and Burgers, 2004). Interestingly, human and *C. elegans* URI are part of a multi-protein complex that contains, among other proteins, the ATPases TIP48 and TIP49 (Gstaiger et al., 2003), which are established components of several chromatin remodeling/modifying complexes, including the human TIP60 HAT complex (Frank et al., 2003). Recently, the *C. elegans* homologs of TIP48 and TIP49, and URI-1 were shown to be required for the process of RNA silencing (Kim et al., 2005). Moreover, our laboratory showed that URI-1 binds a component of the Paf1 complex in human cells, which is important for histone modification and cell cycle control (Yart et al., 2005). Given these links, it is tempting to speculate that at least one function of URI-1 is, directly or indirectly, dedicated to chromatin remodelling and/or replication and repair, and that defects in these processes could possibly explain the endogenous DNA damage in *uri-1*-depleted animals.

Interestingly, *S. cerevisiae rad27* (Tong et al., 2001) is synthetically lethal with the *S. cerevisiae* ortholog of *uri-1* (*bud27*) (Reagan et al., 1995). The human ortholog of *rad27*, the potential

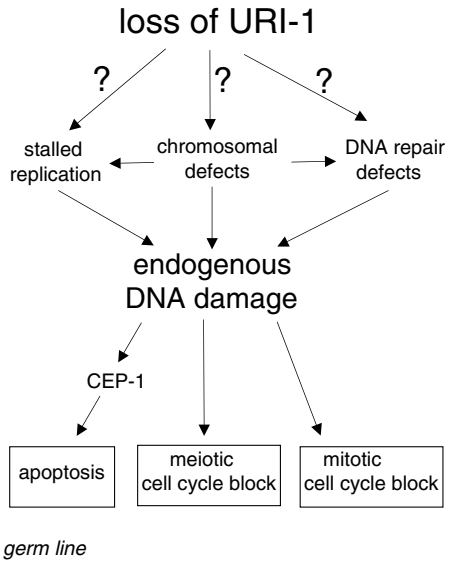

Fig. 7. A proposed model of URI-1 function. Genetic and cell biological analysis show that URI-1 prevents DNA damage and the subsequent activation of the DNA damage signaling pathway by functioning directly or indirectly in DNA damaging processes and/or DNA repair processes. DNA damage caused by deficiency of URI-1 affects germ cells by leading to proliferation arrest in the mitotic region and p53-dependent apoptosis, as well as cell cycle arrest in the meiotic part of the germline. This phenotypes are consistent with reported read outs of the DNA-damage response (Deng et al., 2004; Stergiou and Hengartner, 2004).

cancer susceptibility gene human flap endonuclease 1 (FEN1) (Harrington and Lieber, 1994; Lieber, 1997; Stillman, 1989), is known to have a role in the maintenance of genetic stability in eukaryotic genomes (for reviews, see Henneke et al., 2003; Kucherlapati et al., 2002). It is also known to function in DNA repair (BER, NIR, HR and NHEJ) (Ishchenko et al., 2003; Klungland and Lindahl, 1997; Lieber, 1997; Tishkoff et al., 1997; Wu et al., 1999) and DNA replication, two processes essential for proper proliferation.

In mammalian and yeast cells, URI has been shown to have a central role in the regulation of nutrient-sensitive TOR-dependent gene expression programs. Interestingly, a link between genomic stability and nutrient status has been previously suggested (Fiorentino and Crabtree, 1997; Kurz and Lees-Miller, 2004). One of these reports shows that the yeast dna2 mutant, which displays all of the characteristics of cells blocked at the G_2/M border, can be rescued by the overexpression of the nutrient sensor Tor1p (Fiorentino and Crabtree, 1997). In addition, *dna-2* is a player in cellular processes like germline development and DNA repair in *C. elegans* (Lee et al., 2003) and has been shown to be involved in DNA replication in yeast (Kao et al., 2004). Moreover, a *dna-2* mutant in combination with *mre-11*, a gene that encodes a protein required for meiotic recombination and DNA repair (Chin and Villeneuve, 2001), exhibits a small germline phenotype similar to *uri-1(lf)* (Lee et al., 2003). Finally, mutants of genes implicated in nutrient sensing, starvation and mitochondrial respiratory chain-deficiency in general display a L3 larval arrest (Long et al., 2002; Tsang et al., 2001), similar to the arrest observed in *uri-1(lf)* mutants, pointing to the possibility that the function of URI as a mediator of nutrient signals is conserved in *C. elegans*. The transition from L3 to L4, which entails an increase in mtDNA copy number, has been speculated to involve an energy-sensing decision or checkpoint (Tsang et al., 2001) and is around the developmental time point at which the *uri-1(lf)* proliferation defects emerge. All these data indicate a possible link between nutrient status, DNA metabolism and DNA damage. In this respect, it is interesting to mention that the size of the germ cell nuclei in *uri-1(RNAi)*F1 animals is enlarged (see arrowheads in Fig. 3A), a phenotype that is also observed during radiation-induced cell proliferation arrest and results from growth without proliferation (Gartner et al., 2000). However, unlike the effects of a single γ-irradiation dose, which induces homogeneous increase in size of nuclei, loss of URI-1 function induces heterogeneous enlargement. The different extent of enlargement could indicate that individual cells receive proliferation-blocking stimuli at different times or stages.

In summary, our findings identify a novel role for URI-1 in the maintenance of DNA integrity by affecting directly or indirectly DNA metabolism. As DNA breaks are damaging for cells and bear a mutagenic potential, it will be interesting to test if this novel and essential function of the evolutionary conserved protein URI-1 is conserved in higher organisms. As the mammalian URI-1 ortholog co-exists in a biochemical complex with the human PAF-1 complex, it will be interesting to test if URI-1 maintains DNA stability by affecting the state of chromatin. URI-1 may represents a novel link between the epigenetic regulation of chromatin structure and genomic integrity with implications for human cancer.

We thank M. Gstaiger for his support in the early stages of this work. We also thank all members of the Gotta, Krek and Hengartner laboratories for helpful discussions. We are particularly thankful to S. Ahmed, D. Anastasiou, I. J. Frew, Y. Shi and M. Sohrmann for critical reading of the manuscript and many insightful comments and discussions, and to J. C. Labbé, A. Spilker and C. Dittrich for help with genetics. The rabbit polyconal anti-RAD-51 antibody was generously provided by A. Gartner (Wellcome Trust Biocentre, Dundee, UK). The *uri-1(tm939)* mutant allele was isolated and kindly provided by the NBP-Japan, Mitani Laboratory, Tokyo. The *gld-2(q497) gld-1(q485); unc-32(e189)* strain was kindly provided by J. Kimble (University of Wisconsin, Madison, WI). All other strains used in this paper were provided by the *Caenorhabditis* Genetics Center, which is funded by the National Institute of Health (NIH) National Center for Research Resources (NCRR). This research was supported by a SNF grant (to M.G.) and by the Novartis Foundation (to C.T.P.).

Supplementary material

Supplementary material for this article is available at http://dev.biologists.org/cgi/content/full/133/4/621/DC1

References

Abraham, R. T. (2001). Cell cycle checkpoint signaling through the ATM and ATR kinases. *Genes Dev.* **15**, 2177-2196.

Ahmed, S., Alpi, A., Hengartner, M. O. and Gartner, A. (2001). C. elegans RAD-5/CLK-2 defines a new DNA damage checkpoint protein. *Curr. Biol.* **11**, 1934-1944.

Alpi, A., Pasierbek, P., Gartner, A. and Loidl, J. (2003). Genetic and cytological characterization of the recombination protein RAD-51 in Caenorhabditis elegans. *Chromosoma* **112**, 6-16.

Austin, J. and Kimble, J. (1987). Glp-1 is required in the germ line for regulation of the decision between mitosis and meiosis in C. elegans. *Cell* **51**, 589-599.

Barton, M. K., Schedl, T. B. and Kimble, J. (1987). Gain-of-function mutations of fem-3, a sex-determination gene in Caenorhabditis elegans. *Genetics* **115**, 107-119.

Beanan, M. J. and Strome, S. (1992). Characterization of a germ-line proliferation mutation in C. elegans. *Development* **116**, 755-766.

Boulton, S. J., Gartner, A., Reboul, J., Vaglio, P., Dyson, N., Hill, D. E. and Vidal, M. (2002). Combined functional genomic maps of the C. elegans DNA damage response. *Science* **295**, 127-131.

Brenner, S. (1974). The genetics of Caenorhabditis elegans. *Genetics* **77**, 71-94.

Capowski, E. E., Martin, P., Garvin, C. and Strome, S. (1991). Identification of grandchildless loci whose products are required for normal germ-line development in the nematode Caenorhabditis elegans. *Genetics* **129**,1061-1072.

Chin, G. M. and Villeneuve, A. M. (2001). C. elegans mre-11 is required for meiotic recombination and DNA repair but is dispensable for the meiotic G(2) DNA damage checkpoint. *Genes Dev.* **15**, 522-534.

Cowan, N. J. and Lewis, S. A. (1999). A chaperone with a hydrophilic surface. *Nat. Struct. Biol.* **6**, 990-991.

Deng, X., Hofmann, E. R., Villanueva, A., Hobert, O., Capodieci, P., Veach, D. R., Yin, X., Campodonico, L., Glekas, A., Cordon-Cardo, C. et al. (2004). Caenorhabditis elegans ABL-1 antagonizes p53-mediated germline apoptosis after ionizing irradiation. *Nat. Genet.* **36**, 906-912.

Dernburg, A. F., McDonald, K., Moulder, G., Barstead, R., Dresser, M. and Villeneuve, A. M. (1998). Meiotic recombination in C. elegans initiates by a conserved mechanism and is dispensable for homologous chromosome synapsis. *Cell* **94**, 387-398.

Ehrenhofer-Murray, A. E. (2004). Chromatin dynamics at DNA replication, transcription and repair. *Eur. J. Biochem.* **271**, 2335-2349.

Fiorentino, D. F. and Crabtree, G. R. (1997). Characterization of Saccharomyces cerevisiae dna2 mutants suggests a role for the helicase late in S phase. *Mol. Biol. Cell* **8**, 2519-2537.

Frank, S. R., Parisi, T., Taubert, S., Fernandez, P., Fuchs, M., Chan, H. M., Livingston, D. M. and Amati, B. (2003). MYC recruits the TIP60 histone acetyltransferase complex to chromatin. *EMBO Rep.* **4**, 575-580.

Fraser, A. G., Kamath, R. S., Zipperlen, P., Martinez-Campos, M., Sohrmann, M. and Ahringer, J. (2000). Functional genomic analysis of C. elegans chromosome I by systematic RNA interference. *Nature* **408**, 325-330.

Gartner, A., Milstein, S., Ahmed, S., Hodgkin, J. and Hengartner, M. O. (2000). A conserved checkpoint pathway mediates DNA damage–induced apoptosis and cell cycle arrest in C. elegans. *Mol. Cell* **5**, 435-443.

Geissler, S., Siegers, K. and Schiebel, E. (1998). A novel protein complex promoting formation of functional alpha- and gamma-tubulin. *EMBO J.* **17**, 952-966.

Golden, A., Sadler, P. L., Wallenfang, M. R., Schumacher, J. M., Hamill, D. R., Bates, G., Bowerman, B., Seydoux, G. and Shakes, D. C. (2000). Metaphase to anaphase (mat) transition-defective mutants in Caenorhabditis elegans. *J. Cell Biol.* **151**, 1469-1482.

Gstaiger, M., Luke, B., Hess, D., Oakeley, E. J., Wirbelauer, C., Blondel, M., Vigneron, M., Peter, M. and Krek, W. (2003). Control of nutrient-sensitive transcription programs by the unconventional prefoldin URI. *Science* **302**, 1208-1212.

Hansen, D., Hubbard, E. J. and Schedl, T. (2004). Multi-pathway control of the proliferation versus meiotic development decision in the Caenorhabditis elegans germline. *Dev. Biol.* **268**, 342-357.

Harrington, J. J. and Lieber, M. R. (1994). The characterization of a mammalian DNA structure-specific endonuclease. *EMBO J.* **13**, 1235-1246.
Hartwell, L. H. and Weinert, T. A. (1989). Checkpoints: controls that ensure the order of cell cycle events. *Science* **246**, 629-634.
Helt, C. E., Cliby, W. A., Keng, P. C., Bambara, R. A. and O'Reilly, M. A. (2005). Ataxia telangiectasia mutated (ATM) and ATM and Rad3-related protein exhibit selective target specificities in response to different forms of DNA damage. *J. Biol. Chem.* **280**, 1186-1192.
Henneke, G., Friedrich-Heineken, E. and Hubscher, U. (2003). Flap endonuclease **1**, a novel tumour suppresser protein. *Trends Biochem. Sci.* **28**, 384-390.
Hofmann, E. R., Milstein, S., Boulton, S. J., Ye, M., Hofmann, J. J., Stergiou, L., Gartner, A., Vidal, M. and Hengartner, M. O. (2002). Caenorhabditis elegans HUS-1 is a DNA damage checkpoint protein requiredfor genome stability and EGL-1-mediated apoptosis. *Curr. Biol.* **12**, 1908-1918.
Hope, I. A. (1999). C. elegans: *A Practical Approach*. Oxford: Oxford University Press.
Hsu, J. Y., Sun, Z. W., Li, X., Reuben, M., Tatchell, K., Bishop, D. K., Grushcow, J. M., Brame, C. J., Caldwell, J. A., Hunt, D. F. et al. (2000). Mitotic phosphorylation of histone H3 is governed by Ipl1/aurora kinase and Glc7/PP1 phosphatase in budding yeast and nematodes. *Cell* **102**, 279-291.
Ishchenko, A. A., Sanz, G., Privezentzev, C. V., Maksimenko, A. V. and Saparbaev, M. (2003). Characterisation of new substrate specificities of Escherichia coli and Saccharomyces cerevisiae AP endonucleases. *Nucleic Acids Res.* **31**, 6344-6353.
Kadyk, L. C. and Kimble, J. (1998). Genetic regulation of entry into meiosis in Caenorhabditis elegans. *Development* **125**, 1803-1813.
Kao, H. I., Campbell, J. L. and Bambara, R. A. (2004). Dna2p helicase/nuclease is a tracking protein, like FEN1, for flap cleavage during Okazaki fragment maturation. *J. Biol. Chem.* **279**, 50840-50849.
Kim, J. K., Gabel, H. W., Kamath, R. S., Tewari, M., Pasquinelli, A., Rual, J. F., Kennedy, S., Dybbs, M., Bertin, N., Kaplan, J. M. et al. (2005). Functional genomic analysis of RNA interference in C. elegans. *Science* **308**, 1164-1167.
Kim, Y. C., Lee, M. H., Ryu, S. S., Kim, J. H. and Koo, H. S. (2002). Coaction of DNA topoisomerase IIIalpha and a RecQ homologue during the germ-line mitosis in Caenorhabditis elegans. *Genes Cells* **7**, 19-27.
Klungland, A. and Lindahl, T. (1997). Second pathway for completion of human DNA base excision-repair: reconstitution with purified proteins and requirement for DNase IV (FEN1). *EMBO J.* **16**, 3341-3348.
Koundrioukoff, S., Polo, S. and Almouzni, G. (2004). Interplay between chromatin and cell cycle checkpoints in the context of ATR/ATM-dependent checkpoints. *DNA Repair (Amst.)* **3**, 969-978.
Kucherlapati, M., Yang, K., Kuraguchi, M., Zhao, J., Lia, M., Heyer, J., Kane, M. F., Fan, K., Russell, R., Brown, A. M. et al. (2002). Haploinsufficiency of Flap endonuclease (Fen1) leads to rapid tumor progression. *Proc. Natl. Acad. Sci. USA* **99**, 9924-9929.
Kurz, E. U. and Lees-Miller, S. P. (2004). DNA damage-induced activation of ATM and ATM-dependent signaling pathways. *DNA Repair (Amst.)* **3**, 889-900.
Lambert, S. and Carr, A. M. (2005). Checkpoint responses to replication fork barriers. *Biochimie* **87**, 591-602.
Lee, M. H., Han, S. M., Han, J. W., Kim, Y. M., Ahnn, J. and Koo, H. S. (2003). Caenorhabditis elegans dna-2 is involved in DNA repair and is essential for germ-line development. *FEBS Lett.* **555**, 250-256.
Lettre, G., Kritikou, E. A., Jaeggi, M., Calixto, A., Fraser, A. G., Kamath, R. S., Ahringer, J. and Hengartner, M. O. (2004). Genome-wide RNAi identifies p53-dependent and -independent regulators of germ cell apoptosis in C. elegans. *Cell Death Differ.* **11**, 1198-1203.
Lieber, M. R. (1997). The FEN-1 family of structure-specific nucleases in eukaryotic DNA replication, recombination and repair. *BioEssays* **19**, 233-240.
Lindahl, T. and Wood, R. D. (1999). Quality control by DNA repair. *Science* **286**, 1897-1905.
Long, X., Spycher, C., Han, Z. S., Rose, A. M., Muller, F. and Avruch, J. (2002). TOR deficiency in C. elegans causes developmental arrest and intestinal atrophy by inhibition of mRNA translation. *Curr. Biol.* **12**, 1448-1461.
Majka, J. and Burgers, P. M. (2004). The PCNA-RFC families of DNA clamps and clamp loaders. *Prog. Nucleic Acid Res. Mol. Biol.* **78**, 227-260.
Morrison, A. J. and Shen, X. (2005). DNA repair in the context of chromatin. *Cell Cycle* **4**, 568-571.
Nelson, G. A., Lew, K. K. and Ward, S. (1978). Intersex, a temperature-sensitive mutant of the nematode Caenorhabditis elegans. *Dev. Biol.* **66**, 386-409.
Osborn, A. J., Elledge, S. J. and Zou, L. (2002). Checking on the fork: the DNA-replication stress-response pathway. *Trends Cell Biol.* **12**, 509-516.
Reagan, M. S., Pittenger, C., Siede, W. and Friedberg, E. C. (1995). Characterization of a mutant strain of Saccharomyces cerevisiae with a deletion of the RAD27 gene, a structural homolog of the RAD2 nucleotide excision repair gene. *J. Bacteriol.* **177**, 364-371.
Reddy, K. C. and Villeneuve, A. M. (2004). C. elegans HIM-17 links chromatin modification and competence for initiation of meiotic recombination. *Cell* **118**, 439-452.
Riddle, D. L., Blumenthal, T., Meyer, B. J. and Pries, J. R. (1997). *C. elegans II.* New York: Cold Spring Harbor Laboratory Press.
Sancar, A., Lindsey-Boltz, L. A., Unsal-Kacmaz, K. and Linn, S. (2004). Molecular mechanisms of mammalian DNA repair and the DNA damage checkpoints. *Annu. Rev. Biochem.* **73**, 39-85.
Schumacher, B., Hofmann, K., Boulton, S. and Gartner, A. (2001). The C. elegans homolog of the p53 tumor suppressor is required for DNA damage-induced apoptosis. *Curr. Biol.* **11**, 1722-1727.
Shen, X., Mizuguchi, G., Hamiche, A. and Wu, C. (2000). A chromatin remodelling complex involved in transcription and DNA processing. *Nature* **406**, 541-544.
Smith, M. M. and Levitan, D. J. (2004). The Caenorhabditis elegans homolog of the putative prostate cancer susceptibility gene ELAC2, hoe-1, plays a role in germline proliferation. *Dev. Biol.* **266**, 151-160.
Stergiou, L. and Hengartner, M. O. (2004). Death and more: DNA damage response pathways in the nematode C. elegans. *Cell Death Differ.* **11**, 21-28.
Stillman, B. (1989). Initiation of eukaryotic DNA replication in vitro. *Annu. Rev. Cell Biol.* **5**, 197-245.
Timmons, L., Court, D. L. and Fire, A. (2001). Ingestion of bacterially expressed dsRNAs can produce specific and potent genetic interference in Caenorhabditis elegans. *Gene* **263**, 103-112.
Tishkoff, D. X., Filosi, N., Gaida, G. M. and Kolodner, R. D. (1997). A novel mutation avoidance mechanism dependent on S. cerevisiae RAD27 is distinct from DNA mismatch repair. *Cell* **88**, 253-263.
Tong, A. H., Evangelista, M., Parsons, A. B., Xu, H., Bader, G. D., Page, N., Robinson, M., Raghibizadeh, S., Hogue, C. W., Bussey, H. et al. (2001). Systematic genetic analysis with ordered arrays of yeast deletion mutants. *Science* **294**, 2364-2368.
Tsang, W. Y., Sayles, L. C., Grad, L. I., Pilgrim, D. B. and Lemire, B. D. (2001). Mitochondrial respiratory chain deficiency in Caenorhabditis elegans results in developmental arrest and increased life span. *J. Biol. Chem.* **276**, 32240-32246.
Vainberg, I. E., Lewis, S. A., Rommelaere, H., Ampe, C., Vandekerckhove, J., Klein, H. L. and Cowan, N. J. (1998). Prefoldin, a chaperone that delivers unfolded proteins to cytosolic chaperonin. *Cell* **93**, 863-873.
Wei, Y., Yu, L., Bowen, J., Gorovsky, M. A. and Allis, C. D. (1999). Phosphorylation of histone H3 is required for proper chromosome condensation and segregation. *Cell* **97**, 99-109.
Wu, X., Wilson, T. E. and Lieber, M. R. (1999). A role for FEN-1 in nonhomologous DNA end joining: the order of strand annealing and nucleolytic processing events. *Proc. Natl. Acad. Sci. USA* **96**, 1303-1308.
Yart, A., Gstaiger, M., Wirbelauer, C., Pecnik, M., Anastasiou, D., Hess, D. and Krek, W. (2005). The HRPT2 tumor suppressor gene product parafibromin associates with human PAF1 and RNA polymerase II. *Mol. Cell Biol.* **25**, 5052-5060.

Table S1. Characterization of the spermatogenesis in *uri-1(RNAi)*F1, *glp-1* and *glp-1;uri-1(RNAi)*F1 hermaphrodites at 25°C

Genotype	% defective sperm	Sperm number	*n*
*uri-1(RNAi)*F1*	43±28	12±7	15
glp-1	0±0	7±2	20
*glp-1;uri-1(RNAi)*F1	0±0	6±2	20

Data are mean ± s.d.
n=number of analyzed animals.
*For the *uri-1(RNAi)*F1 worms, we quantified animals with strongly reduced sperm numbers similar to the *glp-1* mutant.

Table S2. Quantification of the effect of control and *uri-1(RNAi)* in the indicated genetic backgrounds at 25°C on germ cell number

	Germ nuclei per gonad arm	
Genotype	Vector control	*uri-1(RNAi)*F1
ced-3	338±56 (*n*=5)	77±36 (*n*=15)
ced-4	352±29 (*n*=5)	90±58 (*n*=15)

Data are mean ± s.d.
n=number of analyzed animals.